



HAL
open science

APC germline hepatoblastomas demonstrate cisplatin-induced intratumor tertiary lymphoid structures

Guillaume Morcrette, Theo Hirsch, Elise Badour, Jill Pilet, Stefano Caruso,
Julien Calderaro, Yoann Martin, Sandrine Imbeaud, Eric Letouzé, Sandra
Rebouissou, et al.

► **To cite this version:**

Guillaume Morcrette, Theo Hirsch, Elise Badour, Jill Pilet, Stefano Caruso, et al.. APC germline hepatoblastomas demonstrate cisplatin-induced intratumor tertiary lymphoid structures. *OncoImmunology*, 2019, 8 (6), pp.e1583547. 10.1080/2162402X.2019.1583547 . inserm-02346879

HAL Id: inserm-02346879

<https://inserm.hal.science/inserm-02346879>

Submitted on 5 Nov 2019

HAL is a multi-disciplinary open access archive for the deposit and dissemination of scientific research documents, whether they are published or not. The documents may come from teaching and research institutions in France or abroad, or from public or private research centers.

L'archive ouverte pluridisciplinaire **HAL**, est destinée au dépôt et à la diffusion de documents scientifiques de niveau recherche, publiés ou non, émanant des établissements d'enseignement et de recherche français ou étrangers, des laboratoires publics ou privés.

APC germline hepatoblastomas demonstrate cisplatin-induced intratumor tertiary lymphoid structures

Guillaume Morcrette, Theo Z Hirsch, Elise Badour, Jill Pilet, Stefano Caruso, Julien Calderaro, Yoann Martin, Sandrine Imbeaud, Eric Letouzé, Sandra Rebouissou, Sophie Branchereau, Sophie Taque, Christophe Chardot, Catherine Guettier, Jean-Yves Scoazec, Monique Fabre, Laurence Brugières & Jessica Zucman-Rossi

To cite this article: Guillaume Morcrette, Theo Z Hirsch, Elise Badour, Jill Pilet, Stefano Caruso, Julien Calderaro, Yoann Martin, Sandrine Imbeaud, Eric Letouzé, Sandra Rebouissou, Sophie Branchereau, Sophie Taque, Christophe Chardot, Catherine Guettier, Jean-Yves Scoazec, Monique Fabre, Laurence Brugières & Jessica Zucman-Rossi (2019) APC germline hepatoblastomas demonstrate cisplatin-induced intratumor tertiary lymphoid structures, *Oncolmmunology*, 8:6, e1583547, DOI: [10.1080/2162402X.2019.1583547](https://doi.org/10.1080/2162402X.2019.1583547)

To link to this article: <https://doi.org/10.1080/2162402X.2019.1583547>



© 2019 The Author(s). Published with license by Taylor & Francis Group, LLC.



[View supplementary material](#)



Published online: 28 Mar 2019.



[Submit your article to this journal](#)



Article views: 638



[View related articles](#)



[View Crossmark data](#)

APC germline hepatoblastomas demonstrate cisplatin-induced intratumor tertiary lymphoid structures

Guillaume Morcrette^{a,b,c}, Theo Z Hirsch^{ib}*, Elise Badour^{*,d}, Jill Pilet^{a,b}, Stefano Caruso^{ib}^{a,b}, Julien Calderaro^{a,b,e,f}, Yoann Martin^{a,b}, Sandrine Imbeaud^{ib}^{a,b}, Eric Letouzé^{ib}^{a,b}, Sandra Rebouissou^{ib}^{a,b}, Sophie Branchereau^g, Sophie Taque^h, Christophe Chardotⁱ, Catherine Guettier^j, Jean-Yves Scoazec^k, Monique Fabre^{*,*l}, Laurence Brugières^{ib}**, and Jessica Zucman-Rossi^{ib}***^{a,b,n}

^aCentre de Recherche des Cordeliers, Functional Genomics of Solid Tumors laboratory, Sorbonne Université, Inserm, USPC, Université Paris Descartes, Université Paris Diderot, Paris, France; ^bLabex Oncolmmunology, Equipe labellisée Ligue Contre le Cancer, Centre de Recherche des Cordeliers, Paris, France; ^cService de Pathologie Pédiatrique, Assistance Publique Hôpitaux de Paris, Hôpital Robert Debré, Paris, France; ^dService de pédiatrie, Centre Hospitalier de la Côte Basque, Bayonne, France; ^eService d'anatomopathologie, Hôpital Henri Mondor, Assistance Publique Hôpitaux de Paris, Créteil, France; ^fInstitut Mondor de Recherche Biomédicale, Université Paris Est Créteil, France; ^gService de chirurgie pédiatrique, Hôpital Bicêtre, Assistance Publique Hôpitaux de Paris, Université Paris-Saclay, Le Kremlin, France; ^hDépartement de Médecine de l'Enfant et l'Adolescent, CHU de Rennes, France; ⁱService de Chirurgie viscérale pédiatrique, Assistance Publique Hôpitaux de Paris, Hôpital Necker-Enfants malades, Paris, France; ^jService d'anatomie et de cytologie pathologiques, Hôpitaux Universitaires Paris Sud, Assistance Publique Hôpitaux de Paris Le Kremlin Bicêtre, Faculté de Médecine Paris Sud, INSERM, Paris, France; ^kService d'anatomie et de cytologie pathologiques, Gustave Roussy Cancer Center, Villejuif, France; ^lService d'anatomie et de cytologie pathologiques, Assistance Publique Hôpitaux de Paris, Hôpital Universitaire Necker-Enfants Malades, Paris, France; ^mDépartement de cancérologie de l'Enfant et l'adolescent, Gustave Roussy Cancer Center, Villejuif, France; ⁿDépartement de cancérologie, Hôpital Européen Georges Pompidou, Assistance Publique Hôpitaux de Paris, Paris, France

ABSTRACT

Hepatoblastoma (HB) is the most common liver cancer in children. We aimed to characterize HB related to APC (Adenomatous Polyposis Coli) germline mutation (APC-HB). This French multicentric retrospective study included 12 APC-HB patients under 5 at diagnosis. Clinical features of APC-HB were compared to the French SIOPEL2-3 cohort of HB patients. Molecular and histopathological analyses of APC-HB were compared to 15 consecutive sporadic HB treated at Bicêtre hospital from 2013 to 2015 (non-APC-HB). APC-HB patients have a peculiar spectrum of germline APC mutations, with no events in the main hotspot of classical APC mutations at codon 1309 ($P < .05$). Compared to sporadic HB, they have similar clinical features including good prognosis since all patients are alive in complete remission at last follow-up. APC-HB are mostly well-limited tumors with fetal predominance and few mesenchymal components. All APC-HB have an activated Wnt/ β -catenin pathway without CTNNB1 mutation, confirming that germline APC and somatic CTNNB1 mutations are mutually exclusive ($P < .001$). Pathological reviewing identified massive intratumor tertiary lymphoid structures (TLS) containing both lymphocytes and antigen-presenting cells in all 11 APC-HB cases who received cisplatin-based neoadjuvant chemotherapy but not in five pre-chemotherapy samples (four paired biopsies and one patient resected without chemotherapy), indicating that these TLS are induced by chemotherapy ($P < .001$). Conclusion: APC-HB show a good prognosis, they are all infiltrated by cisplatin-induced TLS, a feature only retrieved in a minority of non-APC-HB. This suggests that APC inactivation can synergize with cisplatin to induce an immunogenic cell death that initiates an anti-tumor immune response.

ARTICLE HISTORY

Received 28 November 2018
Revised 6 February 2019
Accepted 13 February 2019



KEYWORDS

Pediatric neoplasm;
adenomatous polyposis coli;
antitumor immunity; liver
tumor; immunogenic cell
death

Introduction


Hepatoblastoma (HB) is a rare tumor but the most frequent liver malignancy in children, occurring mostly before 5 y of age. HB incidence is estimated at 1.1 case/1,000,000 of children under 15 y old accounting for approximately 15 new HB cases by year in France. In contrast to adult liver hepatocellular carcinomas that occur on cirrhotic liver in more than 80% of cases, HB usually develops in a normal, non-fibrotic liver. Morphologically, HB tumor cells resemble to immature parenchymal liver cells that are found during embryonal and fetal liver development.

At the molecular level, HB is characterized by CTNNB1 exon 3 mutations or deletions which are detected in 70–80% of the cases.¹ These mutations lead to a stabilization and intracellular accumulation of β -catenin protein. As a consequence, WNT/ β -catenin signaling pathway is activated and induces the expression of target genes like GLUL (coding for glutamine synthetase (GS)) or LGR5 in the tumor cells. Recently, whole exome sequencing studies^{2,3} identified only few additional mutations in HB with a mean rate of three mutations per tumor comparable with other pediatric tumors.

CONTACT Jessica Zucman-Rossi  jessica.zucman-rossi@inserm.fr  INSERM UMR5-1138, Functional genomics of solid tumors (FUNGEST), 27 Rue Juliette Dodu, Paris 75010, France

*Co-first authors, equally contributed

**Co-senior and co-corresponding authors

 Supplemental data for this article can be accessed on the [publisher's website](#).

© 2019 The Author(s). Published with license by Taylor & Francis Group, LLC.

This is an Open Access article distributed under the terms of the Creative Commons Attribution-NonCommercial-NoDerivatives License (<http://creativecommons.org/licenses/by-nc-nd/4.0/>), which permits non-commercial re-use, distribution, and reproduction in any medium, provided the original work is properly cited, and is not altered, transformed, or built upon in any way.

Although most HB is sporadic, several inherited syndromes such as familial adenomatous polyposis (FAP) predispose to HB development. FAP is caused by germline mutations at 5q22 in the *APC* (Adenomatous Polyposis Coli) gene. It is a dominant hereditary disease that mainly causes colonic adenoma growth during adolescence (mean age 16 y) and colon adenocarcinoma in young adults (mean age 39 y) with almost a complete penetrance.⁴ The *APC* protein is a tumor suppressor mostly known for its implication in the so-called destruction complex where it induces the degradation of β -catenin. By disrupting this complex, *APC* inactivating mutations lead to the activation of the Wnt/ β -catenin pathway. However, *APC* also has functions independent of β -catenin, meaning that *APC* and *CTNNB1* mutations are not functionally equivalent.⁵

Patients with FAP have a 750–7500 fold increase relative risk to develop HB, but the prevalence of HB in *APC* mutation carriers is below 3%.⁶ The need for surveillance for HB development in those children is still a matter of debate. Many large North American centers have recommended such a surveillance⁶ whereas in Europe most groups do not recommend surveillance considering the low prevalence of HB in this population² and the high cure rates of patients with HB. Conversely, since FAP is associated with several malignancies (colon, thyroid, brain, bone, soft tissues neoplasms) and can be unknown because of the high proportion of *de novo* mutations,⁴ diagnosing FAP in children with HB is a major issue for the management of the patient and his/her relatives including monitoring colonic adenomas and performing prophylactic surgery before colon adenocarcinoma occurrence in *APC* mutation carriers. Currently, there is still no consensus to perform systematic *APC* genetic screening for children with HB. Detecting specific features of *APC*-HB that could help the management of those patients would further plead for such a screening.

The aim of this study was to identify specific features of *APC*-HB compared to sporadic HB, in order to improve the management of these patients.

Material and methods

APC patients and controls

Germline *APC* mutated hepatoblastoma patients (“*APC*-HB”) were retrieved retrospectively by a systematic screening of Société Française des Cancers de l’Enfant (SFCE) centers that treat all children over France with HB following “Société Internationale d’Oncologie Pédiatrique – Epithelial Liver Tumor Study Group” (SIOPEL) protocols. We identified 12 patients using our criteria of inclusion: development of a HB proven by histology in patients below 5 y old at diagnosis and with a constitutional inactivating *APC* mutation. All the clinical and biological features of the 12 patients were recorded including age at diagnosis, gender, PRETEXT outcome, FAP discovery mode, alpha-fetoprotein (AFP) rate at diagnosis (ng/ml). *APC*-HB patients clinical and biological data were compared with the French cohort of HB patients treated by SIOPEL 2 and 3 protocol between 1996 and 2006 ($n = 76$ after exclusion of four *APC*-HB and six patients older than 5 y). For histological and molecular comparison, the

control group (“non-*APC*-HB”) consisted in 15 consecutive patients who underwent surgery for HB at Bicêtre Hospital (France) between 2012 and 2015, aged less than 5 y and without *APC* germline mutation. All non-*APC*-HB patients were treated by surgical resection after neoadjuvant chemotherapy according to the SIOPEL protocol. For all the patients, parents have signed an informed consent and this study was approved by the appropriate ethics committee (Comité de Protection des Personnes Ile-de-France VII, projects C0-15-003 and PP 16-001) in accordance with the ethical guidelines of the 1975 Declaration of Helsinki.

Pathological reviewing

For each patient tumors, slides were reviewed by four pathologists specialized in pediatric liver diseases (GM, MF, CG, JYS). Tumor pathological features were recorded with at least two independent reviews per feature according to the consensus classification⁷: size, capsule, necrosis, tumor type, component (fetal, pleomorphic fetal, fetal mitotically active, embryonal, cholangioblastic, macrotrabecular; mesenchymal osteoid subtype, mesenchymal spindle cell subtype, teratoid; small cell undifferentiated, Supporting Figure 1A), and mitotic index. Other tumor-specific patterns such as steatosis, clear cells, tumor cholestasis, and pseudoglandular structures were annotated.

Pathological features of tumor-infiltrating leukocytes and tertiary lymphoid structures (TLS) were annotated first on hematein-eosin-safran (HES) slides then characterized by immunohistochemistry (IHC) according to previously published data from the literature.^{9,10} TLS were graded as (1) aggregate (vague lymphoid aggregation), (2) primary follicle (round-shaped nest of lymphocytes without germinal center formation), and (3) secondary follicle (well-formed follicle with clearly identifiable germinal center composed of clear large lymphocytes). Representative images of the TLS observed are available in Supporting Figure 2.

Immunohistochemistry

When formalin-fixed paraffin-embedded tissues were available, immunohistochemical analysis was performed by the immunoperoxidase technique using an automated stainer (Leica Bond system) and visualized with diaminobenzidine. Tumors were analyzed with anti- β -catenin (BD Transduction, clone 14, 610154, 1/300), anti-GS (Bioscience, 1/500) anti-glypican 3 (Zytomed systems, clone 1G12, MSK067-05, 1/100) anti-EPCAM (Abcam, clone MOC-31, 1/200), anti-CK19 (Dako, clone RCK108, 1/100), and ki67 (Dako, clone MIB-1, 1/100). Intratumor inflammatory infiltration was characterized with CD3 (Dako, 1/300), CD20 (Dako, clone L26, 1/50), CD8 (Dako, clone C8/144B, 1/30), CD163 (Novocastra, clone 10D6, 1/600), and anti-DCLamp (Dendritics, clone 1010E1.01, 1/100) antibodies. The abundance of CD3⁺, CD8⁺, CD20⁺, and DCLamp⁺ cells was assessed both within TLS and as isolated tumor-infiltrating leukocytes outside TLS, with the following semi-quantitative scale: score 0, 1, 2, 3, and 4 for none, very low, weak, intermediate, and high density of positive cells, respectively, as in.¹¹

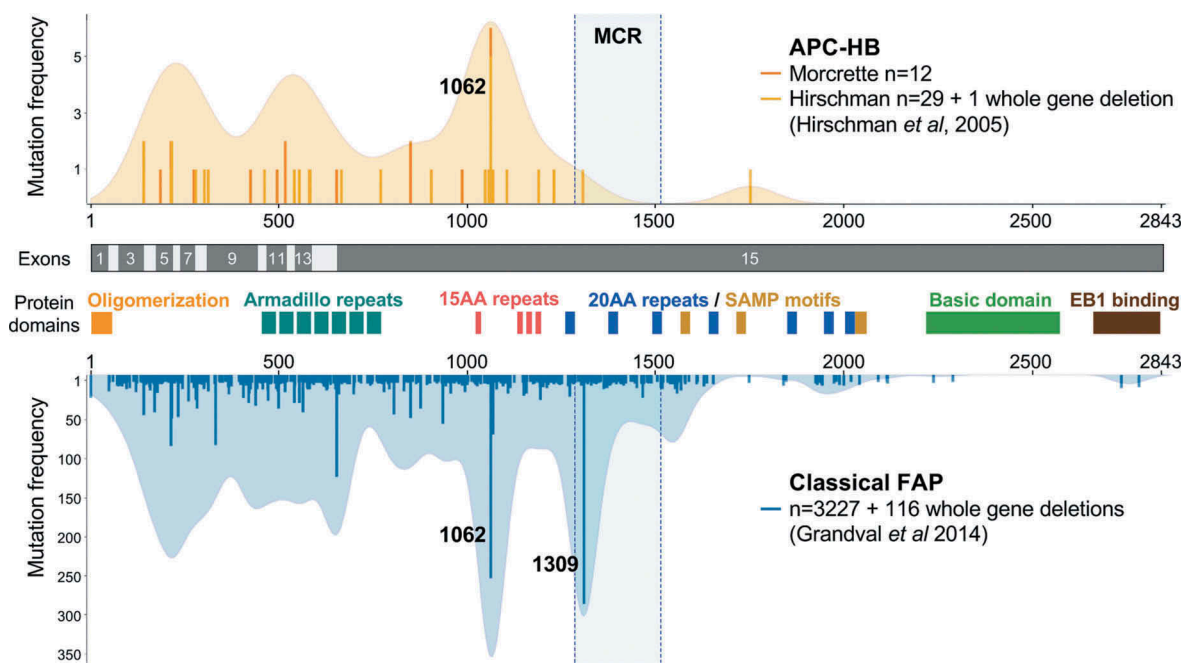


Figure 1. The spectrum of *APC* mutations differs between classical FAP and HB patients.

Lollipop and density plot showing the distribution of *APC* germline mutations. A total of 3343 FAP-related *APC* mutations were obtained from the UMD-APC mutations database (<http://www.umd.be/APC/>, 3717 variants extracted in June 2018 and filtered for keeping only causal and likely causal mutations). Thirty HB-related *APC* mutations were obtained from the publication of Hirschman *et al*⁸ and added to the 12 mutations newly described in this paper. Exons of the *APC* gene and important domains of the APC protein are indicated, including the β -catenin binding domain (15 amino-acid repeats), the β -catenin degradation domain (20 amino-acid repeats), the axin binding domain (SAMP motifs), and the microtubule binding region (basic domain).

Genomic sequencing

Frozen tumor and non-tumor liver tissues were available in 4/12 APC-HB and all the control non-APC-HB. DNA was extracted with Maxwell DNA extraction kit (Promega), and gene mutation was screened by Sanger sequencing for *CTNNB1*, *APC*, *NFE2L2*, and *TERT* promoter (for detailed protocol see¹²). All *APC* germline mutations were confirmed on blood DNA.

Gene expression analysis

When frozen tissues were available, RNA was extracted with Maxwell RNA extraction kit (Promega), and gene expression was analyzed by quantitative reverse-transcriptase PCR (qRT-PCR) with Biomark HD technology (Fluidigm 96.96, San Francisco, California, USA) using protocol previously described.¹³ Expression levels were determined with the $2^{-\Delta\Delta Ct}$ method, using 18S and actin as reference genes for normalization. Full list of the TaqMan probes used is available in Supporting Table 1.

Statistical analyses

Statistical tests and data visualization were performed using R open-source software (R Foundation for Statistical Computing, Vienna, Austria). Analysis has been performed with Fisher exact test for categorical data, Wilcoxon test for continuous data and log-rank test for survival.

Results

Clinical features of APC-HB compared to non-APC-HB

A total of 12 children with APC-HB diagnosed between 1980 and 2016 were retrospectively identified in SFCE centers (Table 1) and compared to the cohort of 76 French HB patients included in SIOPEL protocols between 1996 and 2006 and without known *APC* germline mutation (Table 2). Seven APC-HB patients had a familial FAP history already identified at the time of the HB diagnosis, but none of those tumors were diagnosed by systematic surveillance of *APC* mutation carriers. The diagnosis of FAP was performed after the diagnosis of HB in the five other cases, either as a consequence of a congenital hypertrophy of the retinal pigment epithelium or a colonic polyposis discovered in the mother, or as part of a systematic genetic screening recommended in France since 2013 (Table 1).

Features of the APC-HB patients were comparable to that of the SIOPEL cohort with a non-significant enrichment in male gender (83% vs. 58%) and older age at diagnosis of HB (mean 23.9 vs. 17.8 months), more premature birth (27% vs. 5%) but similar staging of the disease, biological features, and treatment (Table 2). APC-HB had also quite similar clinical features compared to a series of 15 consecutive non-APC-HB surgically treated in Bicêtre Hospital (France) that served as a control group for molecular and histopathological analyses (see below), with this time a significant enrichment in older patients (23.9 vs. 12.9 months, $P = .007$) and lower serum AFP (mean 206,738 vs. 616,198 ng/ml, $P = .006$) (Table 2). At diagnosis, multifocal liver

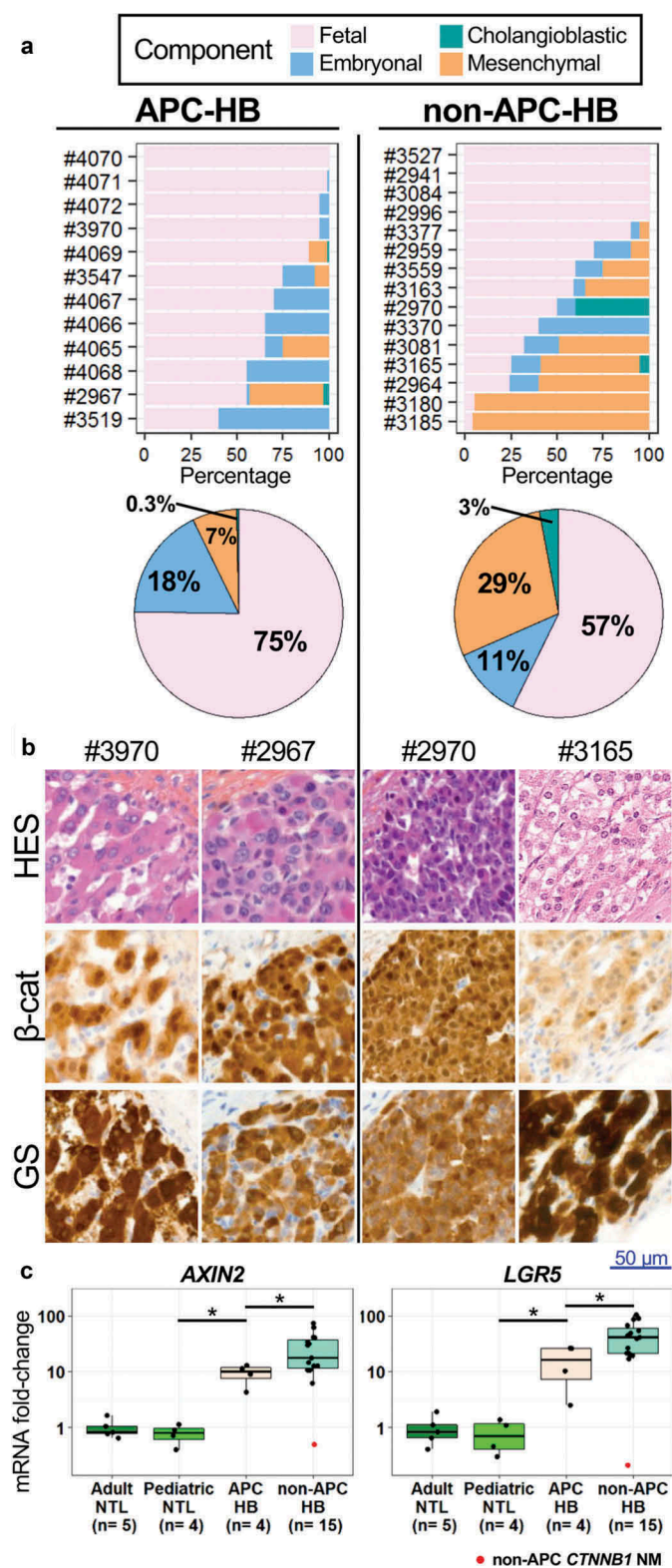


Figure 2. Pathological comparison of APC and non-APC HB.

(a) Histological component distribution assessed by pathological reviewing of APC and non-APC HB. (b) Representative HES and IHC staining of β -catenin (β -cat) and GS within the tumors of APC and non-APC HB patients (high magnification). Lymphocytes without staining are seen in APC-HB. (c) Levels of *AXIN2* and *LGR5* mRNAs assessed by qRT-PCR in APC and non-APC HB as well as in adult and pediatric non-tumor liver (NTL), expressed as a fold-change compared to adult NTL. The non-APC and non-*CTNNB1*-mutated HB sample is marked in red. * $P < .05$ (Wilcoxon test, without taking into account the non-APC *CTNNB1* NM tumor).

nodules were observed in three APC-HB cases (25%) and two patients had lung metastasis. Interestingly two APC-HB patients associated a HB with a hepatocellular adenoma (Supporting Figure 3), a rare benign lesion known to be associated with *APC* germline mutations.¹⁴

All APC-HB patients but one received a neoadjuvant chemotherapy prior to surgical resection based on cisplatin administration, while the remaining patient received arterial embolization without chemotherapy 3 d before surgery. In eight APC-HB with available data, four cycles of chemotherapy induced a decrease in serum AFP in all patients (mean fold-ratio of 156, min–max 9–536, Table 2). Then, 11 patients underwent partial hepatectomy, 1 received liver transplantation. With a mean follow-up of 14 y from diagnosis (min–max: 3.1–36.9 y), all patients are still alive in complete remission. Their disease-specific survival was compared to the SIOPEL cohort (follow-up mean = 4.7 y, min–max: 0.2–9 y) and the Bicêtre cohort (follow-up mean = 3.6 y, min–max: 0.5–5.9 y) (Table 2 and Supporting Figure 4). While seven patients from the SIOPEL arm and two patients from the Bicêtre arm died of their cancer, APC-HB patients achieved 100% of survival. Despite the small size of the sample and the absence of significant difference in the log-rank test ($P = .28$ and $P = .2$ vs. SIOPEL and Bicêtre, respectively), this result suggests that *APC* germline mutation could be associated with good survival. However, these results need to be confirmed in a larger cohort of APC-HB patients.

Spectrum of *APC* germline mutations in HB

In our series of 12 APC-HB patients, we identified nine truncating mutations and three mutations affecting splicing sites in the *APC* gene (Table 1). All these mutations were previously reported as causal in the UMD-*APC* database that includes 3343 FAP mutations (<http://www.umd.be/APC/>).⁴ Adding our 12 French APC-HB germline mutations to the 30 previously reported in the US,⁸ we showed that the spectrum of germline APC-HB patients differs from *APC* mutations in overall FAP (Figure 1). No HB-related *APC* mutations were found at the classical hotspot of mutation at codon 1309, which accounts for 9% of mutations in classical FAP (0/41 vs. 286/3227, $P < .05$), while there was no significant difference for the second FAP-hotspot (codon 1062), which is found mutated in 15% of HB cases compared to 8% in classical FAP (Figure 1). It is also noteworthy that only one HB-related mutation was found in the “somatic mutation cluster region” (MCR, codon 1286–1513) which concentrates 14% of germline mutations in FAP (1/41 vs. 467/3227, $P < .05$) and is associated with a higher number of adenomas and an earlier onset in FAP.^{15,16} Finally, we observed that almost all (98%) HB-related *APC* mutations are strictly 5' to the codon 1309, compared to 80% in classical FAP (40/41 vs. 2566/3227, $P < .01$, Figure 1). These observations confirm that HB phenotype is associated with a particular spectrum of *APC* mutations in FAP.

APC-HB show a predominant fetal phenotype and strong β -catenin activation

Pathological reviewing showed that APC-HB harbor a variety of the typical HB histological components, similar to the 15

Table 1. Features of the 12 APC patients.

HB ID	Age (mths)	Sex	FAP discovery mode	FAP anteriority	gDNA change (GRCh37, chr5)	Protein change
#2967	40	M	FAP Familial follow-up	Familial FAP	112116511del	p.R186Efs*19
#4068	10	F	Colonic polyposis later discovered on mother	Familial FAP	112116592C>T	p.R213*
#3519	56	M	FAP Familial follow-up	Familial FAP	112137070del	p.G275Vfs*18
#3970	14	M	FAP Familial follow-up	Familial FAP	112154999del	p.Q424Rfs*30
#4065	25	M	FAP Familial follow-up	Familial FAP	112162883_112162912delinsTGCTGT	p.T496Mfs*36
#4066	11	M	Colonic polyposis later discovered on mother	Mother <i>de novo</i>	112162945G>A	Splice site (517)
#4070	21	M	FAP Familial follow-up	Familial FAP	112163618A>C	Splice site (517)
#4069	32	F	FAP Familial follow-up	Familial FAP	112170863G>T	Splice site (653)
#3547	17	M	Genetic test APC screening	<i>de novo</i>	112173838_112173841del	p.D849Efs*11
#4072	28	M	CHRPE	Father <i>de novo</i>	112173838_112173841del	p.D849Efs*11
#4071	17	M	FAP Familial follow-up	Familial FAP	112174249T>A	p.Y986*
#4067	19	M	Genetic test APC screening	<i>de novo</i>	112174474_112174478del	p.Q1062*

CHRPE: Congenital hypertrophy of the retinal pigment epithelium.

non-APC-HB from the Bicêtre control group (Figure 2a and Supporting Figure 1). However, APC-HB tend to demonstrate a higher proportion of fetal component (75% vs 57%, $P = .27$) while having a lower proportion of mesenchymal component (7% vs 29%, $P = .09$), particularly of the osteoid component (0.4% vs 18%, $P = .005$) (Figure 2a and Supporting Figure 1). Regarding classical histological features, APC-HB do not differ significantly from non-APC-HB, albeit for a tendency for less pseudoglandular pattern (25% vs 60%, $P = .12$) and more tumor steatosis (50% vs 13%, $P = .09$) (Table 3). All APC-HB tumors had necrosis, ranging from 10% to 95%. Notably, compared to non-APC-HB, all APC-HB but one were well limited (33% vs 89%, $P = .01$), with an intact encapsulated tumor (13% vs 78%, $P = .003$) (Table 3).

In IHC experiments, APC-HB showed a strong Wnt/ β -catenin activation with nuclear β -catenin accumulation in all analyzed tumors (10/10) associated with a strong and diffuse GS expression by tumor fetal component but not in the non-tumor

liver tissues. Of note, the synchronous hepatocellular adenomas observed in two APC-HB patients also had a positive GS staining but no nuclear accumulation of the β -catenin (Supporting Figure 3). The activation of the Wnt/ β -catenin pathway was also observed in 13/14 non-APC-HB (Figure 2b). All non-APC-HB but one (14/15) harbored a *CTNNB1* activating somatic exon 3 mutation/deletion while no *CTNNB1* mutations were found in APC-HB (0/5), confirming previous reports¹⁷ that germline *APC* and somatic *CTNNB1* mutations are mutually exclusive ($P = .0004$, Table 3). No mutations in *TERT* promoter or *NFE2L2* were observed in both groups of HB (Table 3). Among the 24 HB analyzed, the only tumor without nuclear β -catenin staining was from patient #2941 which appears to be neither germline *APC* nor somatic *CTNNB1* mutated.

The assessment by qRT-PCR of the mRNA level of *AXIN2* and *LGR5*, two known Wnt/ β -catenin targets, further showed the activation of this pathway at a higher level in non-APC-HB compared to APC-HB ($P < .05$, Figure 2c).

Table 2. Clinical and biological features of APC-HB compared to SIOPEL-HB cohort and Bicêtre hospital non-APC-HB patients.

Clinical and biological features	APC-HB (n = 12)	SIOPEL-HB (n = 76)	p-val APC vs SIOPEL	Bicêtre non-APC-HB (n = 15)	p-val APC vs non-APC
Age \geq 1 year	10/12 (83%)	49/76 (64%)	0.32	6/15 (40%)	0.047
Mean age in months (range)	23.9 (10–56)	17.8 (0.2–55)	0.11 ^a	12.9 (3–41)	0.007^a
Male sex	10/12 (83%)	44/76 (58%)	0.12	9/15 (60%)	0.24
Prematurity	3/11 (27%)	4/76 (5%)	0.04	1/9 (11%)	0.59
AFP at diag $\geq 1.2 \times 10^6$ ng/ml	1/12 (8%)	5/75 (7%)	1.00	1/14 (7%)	1.00
Mean AFP at diag in ng/ml (range)	2×10^5 (1×10^3 – 1×10^9)	3×10^5 (3×10^2 – 5×10^6)	0.41 ^a	6×10^5 (2×10^4 – 2×10^6)	0.006^a
Mean AFP decrease in fold-ratio (range)*	156 (9–536)	1720 (0.5–37,380)	0.48 ^a	276 (0.8–1471)	0.69 ^a
Metastasis	2/12 (17%)	11/76 (14%)	1.00	2/15 (13%)	1.00
Multifocal tumor	3/12 (25%)	6/76 (8%)	0.10	1/15 (7%)	0.29
PRETEXT I	1/12 (8%)	7/76 (9%)	1.00	0/15 (0%)	0.44
PRETEXT II	5/12 (42%)	33/76 (43%)	1.00	7/15 (47%)	1.00
PRETEXT III	4/12 (33%)	30/76 (39%)	0.76	8/15 (53%)	0.44
PRETEXT IV	2/12 (17%)	6/76 (8%)	0.30	0/15 (0%)	0.19
PRETEXT Tumor Rupture	1/12 (8%)	1/76 (1%)	0.26	0/15 (0%)	0.44
PRETEXT Vascular Invasion	1/12 (8%)	9/76 (12%)	1.00	0/15 (0%)	0.44
PRETEXT Portal vein Invasion	1/12 (8%)	8/76 (11%)	1.00	0/15 (0%)	0.44
PRETEXT Vena cava Invasion	0/12 (0%)	4/76 (5%)	1.00	0/15 (0%)	1.00
Hepatic transplantation	1/12 (8%)	1/70 (1%)	0.27	0/15 (0%)	0.44
R+surgical margin	2/12 (17%)	16/75 (21%)	1.00	3/15 (20%)	1.00
Chemotherapy	11/12 (92%)	76/76 (100%)	0.14	15/15 (100%)	0.44
Cisplatin	11/12 (92%)	76/76 (100%)	0.14	15/15 (100%)	0.44
Carboplatin	5/12 (42%)	24/76 (32%)	0.52	2/14 (14%)	0.19
Doxorubicin	6/12 (50%)	48/76 (63%)	0.53	3/15 (20%)	0.13
Death of disease within 5 y	0/12 (0%)	7/76 (9%)	0.28 ^b	2/15 (13%)	0.20 ^b

The p -value was obtained with Fisher exact test in all cases except for ^a continuous data where Wilcoxon test was used and ^b analysis of survival where Log-rank test was used.

*Ratio of serum AFP at diagnosis to serum AFP after four cycles of chemotherapy.

PRETEXT stands for "pre-treatment assessment of tumor extension"

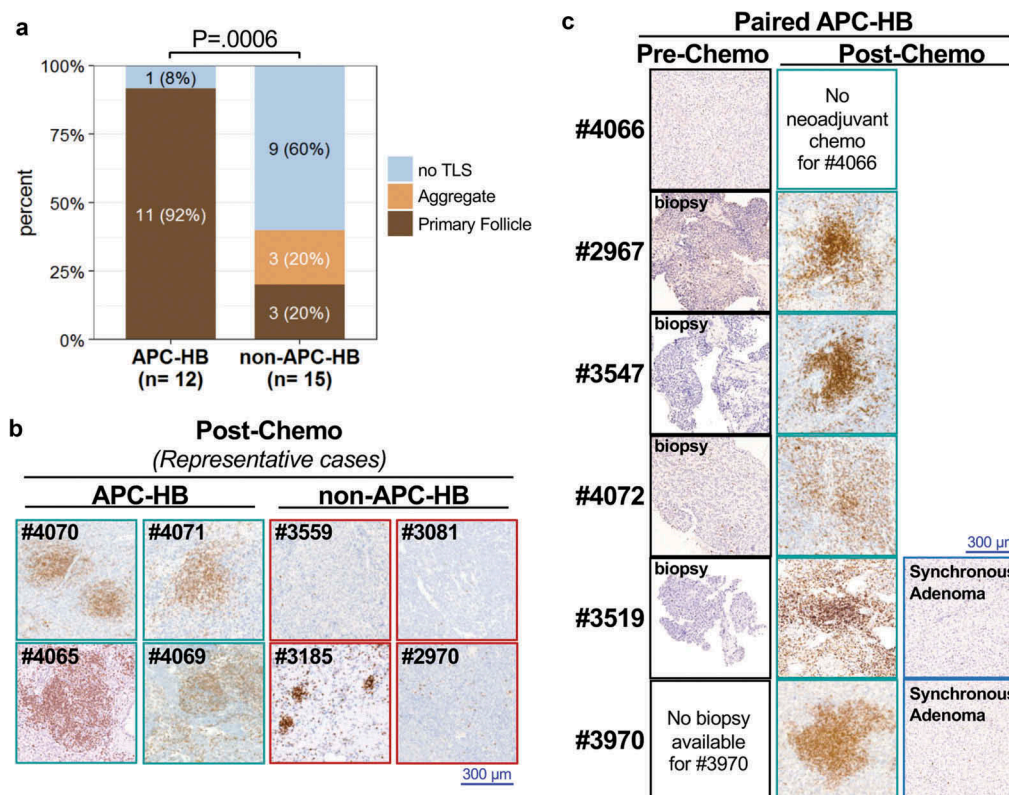


Figure 3. All post-chemotherapy APC-HB have intratumor TLS.

(a) Comparison of intratumor TLS in APC and non-APC HB (trend chi-square test). (b) IHC staining of the T-cell marker CD3 in eight representative post-chemotherapy HBs from four APC and four non-APC mutated patients (low magnification). Primary follicle-type TLS are seen in all four APC-HB while some aggregate-type TLS are present in one non-APC-HB (patient #3185). (c) Comparison of the CD3 staining (low magnification) in paired pre- and post-chemotherapy APC-HB as well as in synchronous adenomas that occurred in both patient #3519 and #3970. Pre-chemotherapy samples were obtained from biopsies for patients #2967, #3547, #4072, and #3519 while it was obtained from curative resection for patient #4066 who did not receive neoadjuvant chemotherapy.

APC-HB are characterized by post-chemotherapy TLS

At pathological reviewing of the HES slides, the most striking pathological feature of APC-HB was the presence of intratumor nests of immune cells evoking TLS that can be categorized in three types regarding their organization (aggregate, primary follicle, or secondary follicle, see Supporting Figure 2 for representative images).¹⁸ Reviewing of both HES and the T cell marker CD3 in IHC revealed that 11 out of 12 APC-HB had intratumor TLS, all of the primary follicle type. Distribution of these lymphoid nests was widespread within the tumor and in direct contact with tumor cells (Figure 3b and Supporting Figure 5 for larger images). In contrast, only 3 out of 15 non-APC-HB showed primary follicle-type TLS, which were restricted to intratumor fibrotic zones for 2/3, while three others harbored aggregate-type TLS (trend chi-squared test $P = .0006$, Figure 3a/b and Supporting Figure 5).

Interestingly, the unique APC-HB patient who did not have TLS in its resected tumor (#4066), was the only one who did not receive neoadjuvant chemotherapy before sampling (Figure 3c). To confirm this association, we analyzed in HES and CD3 IHC the pre-chemotherapy biopsies of four additional APC-HB (#2967, #3547, #4072, and #3519). While the biopsy of patient #4072 showed few isolated intratumor CD3⁺ cells, no TLS were found in any of the four biopsies, in contrast to the paired post-chemotherapy resected tumors of the same patients (Figure 3c).

Noteworthy, in both patients (#3519 and #3970) who developed a hepatocellular adenoma synchronous to their HB, adenoma lesions did not display any TLS after chemotherapy, in contrast to the paired TLS-positive HB (Figure 3c). Thus, intratumor TLS was constantly observed in APC-HB after chemotherapy (0/5 in pre-chemotherapy vs 11/11 in post-chemotherapy, $P = .0002$) but not in the paired benign adenomas (0/2).

To gain further insight into the cellular composition of these intratumor TLS, we performed IHC analysis of different leukocytes markers with a semi-quantitative scale (Figure 4a/B and Table 3). All the TLS in post-chemotherapy APC-HB were highly positive for the T cell markers CD3 and CD8, while they harbored only few B cells positive for CD20, few DC-LAMP⁺ dendritic cells, as well as CD68⁺ macrophages and CD117⁺ mast cells, accounting for an active antigen-presentation within the TLS + tumors (Figure 4a/b). A similar distribution was observed in both aggregate type and primary follicle-type TLS present in six non-APC-HB tumors but with a lower absolute number of immune cells (Figure 4b). Leukocytes were also found as isolated cells outside TLS at various levels in all analyzed post-chemotherapy tumors, including eight non-APC-HB without TLS. Overall, in either APC or non-APC HB tumors, immune cells were predominantly found within TLS (Figure 4b). All non-APC-HB without TLS showed a very low or weak density of intratumor T lymphocytes (CD3⁺ and CD8⁺) while three-eighths of these tumors had no visible CD20⁺ B lymphocytes (Figure 4b).

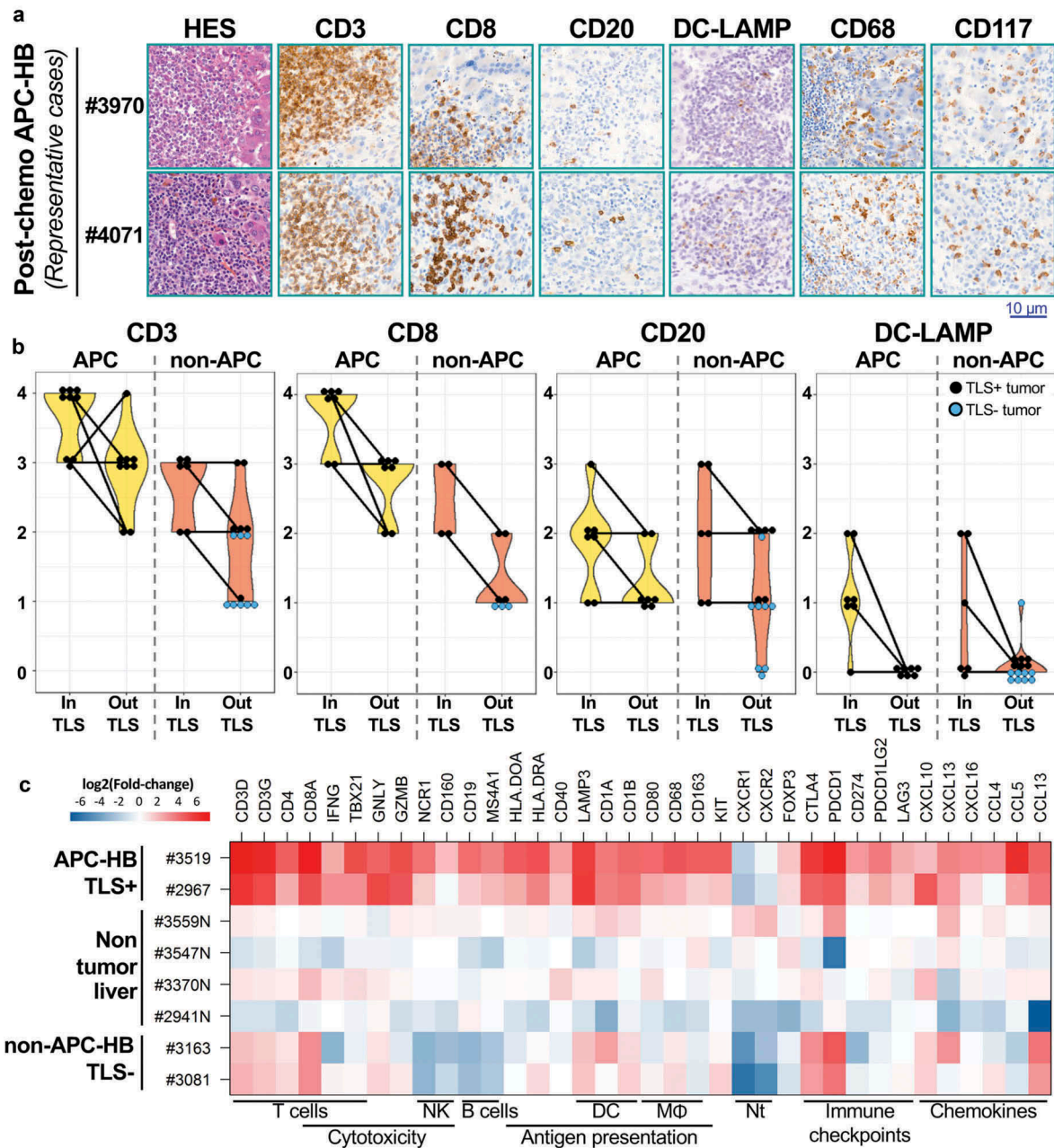


Figure 4. Cellular composition of post-chemotherapy TLS.

(a) Representative HES and IHC staining of markers of T cells (CD3, CD8), B cells (CD20), dendritic cells (DC-LAMP), macrophages (CD68), and mast cells (CD117) within intratumor TLS from APC-HB (high magnification). (b) Semi-quantitative assessment of the abundance of CD3⁺, CD8⁺, CD20⁺, and DC-LAMP⁺ cells within TLS and outside TLS, in post-chemotherapy APC-HB (left panels, yellow violin plots) and non-APC-HB (right panels, orange violin plots). Score 0, 1, 2, 3, and 4 is used for none, very low, weak, intermediate, and high density of positive cells, respectively. Each dot represents one case, black dots are used for TLS \pm tumors while light blue dots are used for TLS-tumors. (c) Heatmap representation of mRNA expression from 36 immune-related genes in APC-HB samples containing TLS, non-APC HB samples without TLS and non-tumor liver samples, obtained by qRT-PCR and expressed as log-transformed fold-change compared to pediatric non-tumor liver. Immune cell types and pathways related to the chosen genes are indicated under the heatmap (NK: natural killer cells; DC: dendritic cells; M Φ : macrophages; Nt: neutrophils).

Of note, DC-LAMP⁺ dendritic cells were almost all identified within TLS. Conversely, CD68⁺ macrophages and CD117⁺ mast cells were not restricted to the TLS but rather spread into the whole tumor, and APC-HB were enriched in mast cells (75% vs 14%, $P = .008$). Of note, in the five pre-chemotherapy APC-HB tumors analyzed, few isolated CD3⁺ lymphocytes were observed but at a weak density for patient #4072 and even lower density for the four others, indicating that the number of lymphocytes outside TLS is also increased after cisplatin treatment.

In order to better characterize the immunological nature of the tumor micro-environment giving rise to the observed TLS, we measured the expression levels of a panel of 36 immune-related genes in two APC-HB tumors with TLS compared to two non-APC-HB tumors without TLS, as well as four non-tumor liver samples (Figure 4c). All immune-related genes were overexpressed in the two TLS⁺ APC-HB samples except *CXCR1* and *CXCR2* whose low expression could reflect the absence of neutrophils.¹⁹ Markers of T cells

Table 3. Histological and molecular features of APC-HB compared to Bicêtre hospital non-APC-HB.

	APC-HB	Non-APC-HB	p-Value
Histological features			
Mean size in cm (range)	5.4 (3.2–6.4)	6.8 (1–14)	0.12
Intact tumor capsule	7/9 (78%)	2/15 (13%)	0.003
Well limited tumor	8/9 (89%)	5/15 (33%)	0.01
Mean tumor necrosis in % (range)	37 (10–95)	36 (0–90)	0.40
Clear cells	1/12 (8%)	1/15 (7%)	1.00
Tumor steatosis	6/12 (50%)	2/15 (13%)	0.09
Tumor cholestasis	0/12 (0%)	0/15 (0%)	1.00
High mitotic index	0/12 (0%)	2/15 (13%)	0.49
Pseudoglandular pattern	3/12 (25%)	9/15 (60%)	0.12
Tertiary lymphoid structure (TLS)	11/12 (92%)	6/15 (40%)	0.01
IHC features			
Nuclear β -catenin	10/10 (100%)	13/14 (93%)	1.00
Strong GS staining	10/10 (100%)	12/14 (86%)	0.49
CD3 in TLS	9/9 (100%)	6/6 (100%)	1.00
CD8 in TLS	7/7 (100%)	4/4 (100%)	1.00
CD20 in TLS	7/7 (100%)	6/6 (100%)	1.00
DC-LAMP in TLS	6/7 (86%)	3/6 (50%)	0.27
Molecular features			
<i>CTNNB1</i> exon 3 mutated/deleted	0/5 ^a (0%)	14/15 (93%)	0.0004
<i>TERT</i> promoter mutated	0/4 (0%)	0/15 (0%)	1.00
<i>NFE2L2</i> mutated	0/5 ^a (0%)	0/15 (0%)	1.00

^a *CTNNB1* and *NFE2L2* mutational status for one case was obtained from Cairo et al., 2008, case number HB170.

such as the genes coding for CD3, CD4, and CD8 were also slightly expressed in non-APC-HB samples reflecting the presence of a few isolated T cells in those tumors. Conversely, markers of T cell activation and cytotoxicity such as *IFNG*, *TBX21*, *GNLY*, and *GZMB* were only found overexpressed in APC-HB samples, while markers of natural killer and B cells were down-regulated in non-APC-HB samples. Genes coding for various immune checkpoints receptors and ligands such as *CTLA4*, *PD-1/PD-L1* were all overexpressed in APC-HB samples, whereas in non-APC-HB only *CTLA4* and *PDCD1* receptors were expressed. Finally, we observed in APC-HB an overexpression of various chemokines of the CCL and CXCL family, which have been associated with lymphocyte recruitment and entry into TLS.²⁰

Discussion

In this study, we compared APC-HB to both classical FAP patients and sporadic non-APC-HB patients, with two main findings: (i) FAP patients who develop HB have a peculiar *APC* mutation spectrum, and (ii) APC-HB patients are characterized by a good survival and a massive tumor infiltration by leukocytes organized in TLS in response to cisplatin-based chemotherapy.

Regarding *APC* mutations, our observation is a statistical confirmation of 10 y old hypothesis about a different spectrum in HB compared to classical FAP.⁸ We observed a complete absence of mutations in the classical FAP hotspot at codon 1309 in APC-HB patients ($P < .05$), a feature also found in the recent meta-analysis of APC-HB spectrum of mutations.⁶ Genotype–phenotype correlations have been reported in FAP for a long time, with mutations localized in some regions of the gene being associated with the severity of the polyposis or with some extra-colonic features such as desmoid tumors or congenital hypertrophy of the retinal pigment epithelium.⁴ In APC-HB, the exclusion of mutations

in the 1309 codon and in the MCR may relate to the need for a fine-tuning of the activation of the Wnt/ β -catenin pathway in HB tumorigenesis, as it has been proposed for colorectal adenoma.²¹ It may also result from the implication in HB development of *APC* functions beyond the Wnt/ β -catenin pathway,⁵ which could explain our present observation of phenotypic differences between APC-HB and *CTNNB1* mutated non-APC-HB.

Compared to sporadic non-APC-HB patients (the SIOPEL series of 76 French patients as well as the series of 15 patients resected in Bicêtre hospital), APC-HB patients showed quite similar clinical and biological features (Table 2), as it has been reported in a recent retrospective analysis in the US²² and in the meta-analysis of the literature.⁶ In concordance with those studies, APC-HB patients appeared to be slightly older and enriched in the male gender, but none of these features allowed a clinical-based identification of FAP patients. This pleads for a systematic screening for *APC* mutations in HB patients even in the absence of familial history of tumors, since 25–30% of FAP cases arise from a *de novo* mutation.⁴ Such a screening leading to the surveillance of FAP-related neoplasms in *APC* mutation carriers is of major importance for the patient and its relatives. Furthermore, a screening of germline *APC* mutations in large cohorts would be useful to statistically validate our observation of a good survival of APC-HB patients, since the small sample size and the absence of events did not allow our analysis to reach significance ($P = .28$ and $P = .2$ vs. SIOPEL and Bicêtre cohorts, respectively).

The good prognosis of the APC-HB, with a complete remission in all the cases, was associated with chemotherapy-induced intratumor follicle-type TLS in all tumors, a feature only retrieved in 20% of non-APC-HB. This suggests that *APC* alterations have a major role in the induction of an active tumor immune response after cisplatin chemotherapy. Indeed, TLS are defined as lymphoid aggregates forming in response to permanent chronic inflammation, such as chronic infection, autoimmune disease, graft rejection, and cancer. Intratumor TLS can be a witness of an active anti-tumor immune response and have been associated with a good prognosis in a lot of different adult cancers¹⁸ including hepatocellular carcinomas.²³ According to the literature, this work is the first formal description of TLS per-se in pediatric neoplasms. However, intratumor structures resembling secondary lymphoid follicles have been previously described in a subgroup of neuroblastomas associated with the opsoclonus-myoclonus syndrome.²⁴ This rare paraneoplastic autoimmune disorder is of excellent prognosis for neuroblastoma patients, including those with an unfavorable genomic profile, highlighting that an immune response might be involved in tumor control.²⁵

All 11 post-chemotherapy APC-HB had TLS of the primary follicle type with a high density of CD3⁺ T cells but fewer CD20⁺ B cells, and without clear germinal center, indicative of an incomplete maturation. The conjoint observation of DC-LAMP⁺ dendritic cells and CD3⁺ T cells in the TLS may reflect antigen-presentation within the tumor and could be indicative of the implementation of an effective anti-tumor immune response since dendritic cells inside TLS is of good prognosis in tumors such as non-small-cell lung cancer¹¹ or clear cell renal cell carcinoma.²⁶

While it has been known for a long time that chemotherapy can increase the number of tumor-infiltrating lymphocytes in different neoplasms such as breast²⁷ or ovarian cancer,²⁸ the effect of neoadjuvant chemotherapy on TLS is poorly documented. In different types of lung cancers,^{29,30} intratumor TLS have been described both in the presence and the absence of chemotherapy. It was further shown that lung squamous cell carcinoma patients have less germinal centers in their TLS if they received cisplatin-based neoadjuvant chemotherapy, but the chemotherapy was co-administered with corticosteroids that could have a direct inhibitor effect on germinal center maturation.³⁰

To our knowledge, our observation is the first description of chemotherapy-induced TLS formation with paired pre-chemotherapy biopsies as a control, indicating that chemotherapy induces a peculiar immune response. This could involve the so-called immunogenic cell death (ICD), a class of controlled cell death processes that produce damage-associated molecular patterns which can act as adjuvants for initiating the immune response via the recruitment and activation of dendritic cells.³¹ In this regard, it is noteworthy that patient #4066, the only APC-HB patient who did not receive neoadjuvant chemotherapy, had some zones of ischemic-related necrosis induced by arterial embolization in its tumor without any TLS at proximity. This indicates that necrosis is not sufficient to induce the formation of intratumor TLS and highlights the fact that cisplatin-based chemotherapy induces a specific type of cell death related to the immune response. The fact that the synchronous hepatocellular adenomas of two APC-HB patients had no TLS while being from the same surgical specimen than TLS⁺ HB further emphasizes the link between cisplatin-related cell death and TLS, since those two adenomas did not respond to chemotherapy. However, we cannot exclude the fact that this difference in immune response would arise from a difference in antigenicity, since the HB tumors may express neoantigens that are absent in the synchronous adenomas.

All 11 APC-HB patients who went through neoadjuvant chemotherapy received cisplatin, even though some patients also received carboplatin and doxorubicin. Previous studies have shown that cisplatin alone has an incomplete ability to provoke ICD: while it does induce the release of dendritic cells activators such as the HMGB1 protein, it still misses a critical step, the translocation of calreticulin to the membrane,³² which acts as an “eat-me” signal for professional antigen-presenting cells.³¹ This missing step can be compensated by the use of cisplatin in combination with inducers of endoplasmic reticulum stress such as thapsigargin³³ or pyridoxine³⁴ or with the IL8 ortholog Cxcl2³⁵ to induce ICD *in vitro* and *in vivo*. We may thus hypothesize that some mechanism occurring in APC-HB tumor cells is similarly able to compensate for the missing steps of cisplatin in the process of ICD, which would explain why all chemotherapy-treated APC-HB tumors had follicle-type TLS contrary to only 3/15 non-APC-HB. Since most non-APC-HB tumors have *CTNNB1* activating mutations, this hypothetical mechanism could be linked to APC functions not related to the activation of the Wnt/ β -catenin pathway, such as its involvement in cytoskeleton, cell cycle, apoptosis, or genomic stability.⁵ Finally, anticancer immune effects of chemotherapy can be modulated by gut microbiota³⁶ and specific bacterial biofilms selected in FAP patients could interfere with treatment efficacy in APC-HB.³⁷

In conclusion, since APC-HB are associated with a good survival and cisplatin post-chemotherapy active immune response, APC genetic screening of HB patients may help to adapt tumor treatment and avoid unnecessary intensive chemotherapy in these patients. A potential synergic role of anti-tumor immune reinforcement could be tested for HB patients in future clinical trials.

Abbreviations

AFP	Alpha-Fetoprotein
APC	Adenomatous Polyposis Coli
FAP	Familial Adenomatous Polyposis
GS	Glutamine Synthetase
HB	Hepatoblastoma
HES	Hematein-Eosin-Safran
ICD	Immunogenic Cell Death
IHC	Immunohistochemistry
MCR	Mutation Cluster Region
TLS	Tertiary Lymphoid Structure

Acknowledgments

We thank all the clinicians, radiologists and pathologists who participated to this work: Prs. Frédéric Gauthier and Hélène Martelli, Drs. Florent Guérin, Danièle Pariente, Stéphanie Franchi-Abella and Charlotte Mussini; Katia Posseme, Martine Prsle, Véronique Bruna, Delphine Colmant, Marie Josée Redon and Olivier Trassard (CHU Bicêtre, AP-HP, Le Kremlin Bicêtre), Pr Dominique Berrebi; Louis Tournier, Pascal Blain, Elodie Borghesi, Muriel Mateo-Gajardo, Sébastien Carrera, Carole Martignac and Maxette Pierin (CHU Robert Debré, AP-HP, Paris), Dr. Louise Galmiche and Gisèle Le Gall (CHU Necker Enfants Malades, AP-HP, Paris), Pr. Aurore Coulomb-L'hermine, Drs. Sabah Boudjemaa, Sylvie Fasola, Jean Donadieu, and Hélène Boutroux-Darlane (CHU Trousseau, AP-HP, Paris), Drs. Isabelle Aerts and Paul Freneaux (Institut Curie, Paris), Brenda Mallon (Institut Gustave Roussy, Villejuif), Pr. Jean-François Mosnier and Dr. Estelle Thebaud (CHU Nantes), Dr. Bruno Turlin (CHU Rennes), Pr. Yves Perel (CHU Bordeaux), Pr. Jannick Selves (CHU Toulouse), Dr. Cécile Dumesnil and Arnaud François (CHU Rouen), Drs. Claire Hoyoux and Albert Thiry (CHU Liège, Belgium), and Dr. Rudolf Maibach (University of Bern, Switzerland) who provided data from French patients included in SIOPEL 2 and 3 trials. We thank the Paris Sud Tissue bank (CRB PARIS SUD BB-0033-00089) and HEPATOBIO database and the help of the department of biostatistics of Gustave Roussy.

Author contributions

GM, MF, CG, and J-YS provided samples and pathological reviewing. GM, EB, LB, SB, ST, and CC provided samples and clinical information. JZ-R, JC, EL, LB, MF, and SR participated to the study concept and design. GM, JP, and YM generated experimental data. TZH, SC, and SI performed statistical analyses. JZ-R, MF, and LB designed and coordinated the overall study. JZ-R and LB obtained funding for the study. TZH, GM, and JZ-R wrote the manuscript. All authors participated to the critical revision of the manuscript.

Disclosure of Potential Conflicts of Interest


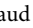
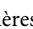
Authors have no conflict of interest to declare.

Funding

FUNGEST team is supported by the Ligue Nationale contre le Cancer (Equipe Labellisée), Labex OncoImmunology (investissement d'avenir), Coup d'Elan de la Fondation Bettencourt-Shueller, the SIRIC CARPEM, Fondation Mérieux, SFCE (Société Française de Lutte Contre les Cancers et les Leucémies de l'Enfant), Fédération Enfants Santé, Etoile de Martin,

l'Association Hubert Gouin « Enfance et Cancer ». GM was supported by CARPEM. TZH was supported by Région Ile de France and then Fondation d'Entreprise Bristol-Myers Squibb pour la Recherche en Immuno-Oncologie. JP is supported by the Fondation Pour La Recherche Médicale, FRM grant number: ECO20170637540.

ORCID

Theo Z Hirsch  <http://orcid.org/0000-0003-4428-2997>
 Stefano Caruso  <http://orcid.org/0000-0002-6319-3642>
 Sandrine Imbeaud  <http://orcid.org/0000-0001-8439-6732>
 Eric Letouzé  <http://orcid.org/0000-0002-6369-2839>
 Sandra Rebouissou  <http://orcid.org/0000-0003-0188-2271>
 Laurence Brugières  <http://orcid.org/0000-0002-7798-6651>
 Jessica Zucman-Rossi  <http://orcid.org/0000-0002-5687-0334>

References

- Cairo S, Armengol C, De Reyniès A, Wei Y, Thomas E, Renard C-A, Goga A, Balakrishnan A, Semeraro M, Gresh L, et al. Hepatic stem-like phenotype and interplay of Wnt/beta-catenin and Myc signaling in aggressive childhood liver cancer. *Cancer Cell*. 2008;14(6):471–484. doi:10.1016/j.ccr.2008.11.002.
- Achatz MI, Porter CC, Brugières L, Druker H, Frebourg T, Foulkes WD, Kratz CP, Kuiper RP, Hansford JR, Hernandez HS, et al. Cancer screening recommendations and clinical management of inherited gastrointestinal cancer syndromes in childhood. *Clin Cancer Res*. 2017;23(13):e107–e114. doi:10.1158/1078-0432.CCR-17-0790.
- Sumazin P, Chen Y, Treviño LR, Sarabia SF, Hampton OA, Patel K, Mistretta T-A, Zorman B, Thompson P, Heczey A, et al. Genomic analysis of hepatoblastoma identifies distinct molecular and prognostic subgroups. *Hepatology*. 2017;65(1):104–121. doi:10.1002/hep.28888.
- Grandval P, Blayau M, Buisine M-P, Coulet F, Maugard C, Pinson S, Remenieras A, Tinat J, Uhrhammer N, Bérout C, et al. The UMD-APC database, a model of nation-wide knowledge base: update with data from 3,581 variations. *Hum Mutat*. 2014;35(5):532–536. doi:10.1002/humu.22539.
- Hankey W, Frankel WL, Groden J. Functions of the APC tumor suppressor protein dependent and independent of canonical WNT signaling: implications for therapeutic targeting. *Cancer Metastasis Rev*. 2018;37(1):159–172. doi:10.1007/s10555-017-9725-6.
- Trobaugh-Lotrario AD, López-Terrada D, Li P, Feusner JH. Hepatoblastoma in patients with molecularly proven familial adenomatous polyposis: clinical characteristics and rationale for surveillance screening. *Pediatr Blood Cancer*. 2018;65(8):e27103. doi:10.1002/pbc.27103.
- López-Terrada D, Alaggio R, de Dávila MT, Czauderna P, Hiyama E, Katzenstein H, Leuschner I, Malogolowkin M, Meyers R, Ranganathan S, et al. Towards an international pediatric liver tumor consensus classification: proceedings of the Los Angeles COG liver tumors symposium. *Mod Pathol*. 2014;27(3):472–491. doi:10.1038/modpathol.2013.80.
- Hirschman BA, Pollock BH, Tomlinson GE. The spectrum of APC mutations in children with hepatoblastoma from familial adenomatous polyposis kindreds. *J Pediatr*. 2005;147(2):263–266. doi:10.1016/j.jpeds.2005.04.019.
- Murakami J, Shimizu Y, Kashii Y, Kato T, Minemura M, Okada K, Nambu S, Takahara T, Higuchi K, Maeda Y, et al. Functional B-cell response in intrahepatic lymphoid follicles in chronic hepatitis C. *Hepatology*. 1999;30(1):143–150. doi:10.1002/hep.510300107.
- Finkin S, Yuan D, Stein I, Taniguchi K, Weber A, Unger K, Browning JL, Goossens N, Nakagawa S, Gunasekaran G, et al. Ectopic lymphoid structures function as microniches for tumor progenitor cells in hepatocellular carcinoma. *Nat Immunol*. 2015;16(12):1235–1244. doi:10.1038/ni.3290.
- Dieu-Nosjean M-C, Antoine M, Danel C, Heudes D, Wislez M, Poulot V, Rabbe N, Laurans L, Tartour E, de Chaisemartin L, et al. Long-term survival for patients with non-small-cell lung cancer with intratumoral lymphoid structures. *J Clin Oncol*. 2008;26(27):4410–4417. doi:10.1200/JCO.2007.15.0284.
- Nault JC, Mallet M, Pilati C, Calderaro J, Bioulac-Sage P, Laurent C, Laurent A, Cherqui D, Balabaud C, Zucman-Rossi J, et al. High frequency of telomerase reverse-transcriptase promoter somatic mutations in hepatocellular carcinoma and preneoplastic lesions. *Nat Commun*. 2013;4(May):2218. doi:10.1038/ncomms3218.
- Rebouissou S, Franconi A, Calderaro J, Letouzé E, Imbeaud S, Pilati C, Nault J-C, Couchy G, Laurent A, Balabaud C, et al. Genotype-phenotype correlation of CTNNB1 mutations reveals different β -catenin activity associated with liver tumor progression. *Hepatology*. 2016;64(6):2047–2061. doi:10.1002/hep.28638.
- Gupta A, Sheridan RM, Towbin A, Geller JI, Tiao G, Bove KE. Multifocal hepatic neoplasia in 3 children with APC gene mutation. *Am J Surg Pathol*. 2013;37(7):1058–1066. doi:10.1097/PAS.0b013e31828aeb18.
- Miyoshi Y, Nagase H, Ando H, Horii A, Ichii S, Nakatsuru S, Aoki T, Miki Y, Mori T, Nakamura Y. Somatic mutations of the APC gene in colorectal tumors: mutation cluster region in the APC gene. *Hum Mol Genet*. 1992;1:229–233.
- Nugent KP, Phillips RK, Hodgson SV, Cottrell S, Smith-Ravin J, Pack K, Bodmer WF. Phenotypic expression in familial adenomatous polyposis: partial prediction by mutation analysis. *Gut*. 1994;35:1622–1623.
- Dubbink HJ, Hollink IHM, Avenca Valente C, Wang W, Liu P, Doukas M, van Noesel MM, Dinjens WNM, Wagner A, Smits R. A novel tissue-based β -catenin gene and immunohistochemical analysis to exclude familial adenomatous polyposis among children with hepatoblastoma tumors. *Pediatr Blood Cancer*. 2018;65(6):e26991. doi:10.1002/pbc.26991.
- Dieu-Nosjean M-C, Giraldo NA, Kaplon H, Germain C, Fridman WH, Sautès-Fridman C. Tertiary lymphoid structures, drivers of the anti-tumor responses in human cancers. *Immunol Rev*. 2016;271(1):260–275. doi:10.1111/imr.12405.
- Becht E, Giraldo NA, Lacroix L, Buttard B, Elarouci N, Petitprez F, Selves J, Laurent-Puig P, Sautès-Fridman C, Fridman WH, et al. Estimating the population abundance of tissue-infiltrating immune and stromal cell populations using gene expression. *Genome Biol*. 2016;17(1):218. doi:10.1186/s13059-016-1070-5.
- Sautès-Fridman C, Lawand M, Giraldo NA, Kaplon H, Germain C, Fridman WH, Dieu-Nosjean M-C. Tertiary lymphoid structures in cancers: prognostic value, regulation, and manipulation for therapeutic intervention. *Front Immunol*. 2016;7(OCT):1–11. doi:10.3389/fimmu.2016.00407.
- Albuquerque C, Breukel C, van der Lijst R, Fidalgo P, Lage P, Slors FJM, Leitão CN, Fodde R, Smits R. The “just-right” signaling model: APC somatic mutations are selected based on a specific level of activation of the beta-catenin signaling cascade. *Hum Mol Genet*. 2002;11(13):1549–1560. doi:10.1093/hmg/11.13.1549.
- Yang A, Sisson R, Gupta A, Tiao G, Geller JI. Germline APC mutations in hepatoblastoma. *Pediatr Blood Cancer*. 2018;65(4):e26892. doi:10.1002/pbc.26892.
- Calderaro J, Petitprez F, Becht E, Laurent A, Hirsch TZ, Rousseau B, Luciani A, Amaddeo G, Derman J, Charpy C, et al. Intra-tumoral tertiary lymphoid structures are associated with a low risk of early recurrence of hepatocellular carcinoma. *J Hepatol*. 2019;70(1):58–65. doi:10.1016/j.jhep.2018.09.003.
- Gambini C, Conte M, Bernini G, Angelini P, Pession A, Paolucci P, Donfrancesco A, Veneselli E, Mazzocco K, Tonini GP, et al. Neuroblastic tumors associated with opsoclonus-myoclonus syndrome: histological, immunohistochemical and molecular features of 15 Italian cases. *Virchows Arch*. 2003;442(6):555–562. doi:10.1007/s00428-002-0747-1.
- Hero B, Clement N, Øra I, Pierron G, Lapouble E, Theissen J, Pasqualini C, Valteau-Couanet D, Plantaz D, Michon J, et al. Genomic profiles of neuroblastoma associated with opsoclonus

- myoclonus syndrome. *J Pediatr Hematol Oncol.* 2018;40(2):93–98. doi:10.1097/MPH.0000000000000976.
26. Giraldo NA, Becht E, Pagès F, Skliris G, Verkarre V, Vano Y, Mejean A, Saint-Aubert N, Lacroix L, Natario I, et al. Orchestration and prognostic significance of immune checkpoints in the microenvironment of primary and metastatic renal cell cancer. *Clin Cancer Res.* 2015;21(13):3031–3040. doi:10.1158/1078-0432.CCR-14-2926.
 27. Demaria S, Volm MD, Shapiro RL, Yee HT, Oratz R, Formenti SC, Muggia F, Symmans WF. Development of tumor-infiltrating lymphocytes in breast cancer after neoadjuvant paclitaxel chemotherapy. *Clin Cancer Res.* 2001;7:3025–3030.
 28. Lo CS, Sanii S, Kroeger DR, Milne K, Talhouk A, Chiu DS, Rahimi K, Shaw PA, Clarke BA, Nelson BH. Neoadjuvant chemotherapy of ovarian cancer results in three patterns of tumor-infiltrating lymphocyte response with distinct implications for immunotherapy. *Clin Cancer Res.* 2017;23(4):925–934. doi:10.1158/1078-0432.CCR-16-1433.
 29. Germain C, Gnjjatic S, Tamzalit F, Knockaert S, Remark R, Goc J, Lepelley A, Becht E, Katsahian S, Bizouard G, et al. Presence of B cells in tertiary lymphoid structures is associated with a protective immunity in patients with lung cancer. *Am J Respir Crit Care Med.* 2014;189(7):832–844. doi:10.1164/rccm.201309-1611OC.
 30. Siliņa K, Soltermann A, Attar FM, Casanova R, Uckelely ZM, Thut H, Wandres M, Isajevs S, Cheng P, Curioni-Fontecedro A, et al. Germinal centers determine the prognostic relevance of tertiary lymphoid structures and are impaired by corticosteroids in lung squamous cell carcinoma. *Cancer Res.* 2018;78(5):1308–1320. doi:10.1158/0008-5472.CAN-17-1987.
 31. Galluzzi L, Buqué A, Kepp O, Zitvogel L, Kroemer G. Immunogenic cell death in cancer and infectious disease. *Nat Rev Immunol.* 2017;17(2):97–111. doi:10.1038/nri.2016.107.
 32. Tesniere A, Schlemmer F, Boige V, Kepp O, Martins I, Ghiringhelli F, Aymeric L, Michaud M, Apetoh L, Barault L, et al. Immunogenic death of colon cancer cells treated with oxaliplatin. *Oncogene.* 2010;29(4):482–491. doi:10.1038/onc.2009.356.
 33. Martins I, Kepp O, Schlemmer F, Adjemian S, Tailler M, Shen S, Michaud M, Menger L, Gdoura A, Tajeddine N, et al. Restoration of the immunogenicity of cisplatin-induced cancer cell death by endoplasmic reticulum stress. *Oncogene.* 2011;30(10):1147–1158. doi:10.1038/onc.2010.500.
 34. Aranda F, Bloy N, Pesquet J, Petit B, Chaba K, Sauvat A, Kepp O, Khadra N, Enot D, Pfirschke C, et al. Immune-dependent anti-neoplastic effects of cisplatin plus pyridoxine in non-small-cell lung cancer. *Oncogene.* 2015;34(23):3053–3062. doi:10.1038/onc.2014.234.
 35. Sukkurwala AQ, Martins I, Wang Y, Schlemmer F, Ruckstuhl C, Durchschlag M, Michaud M, Senovilla L, Sistigu A, Ma Y, et al. Immunogenic calreticulin exposure occurs through a phylogenetically conserved stress pathway involving the chemokine CXCL8. *Cell Death Differ.* 2014;21(1):59–68. doi:10.1038/cdd.2013.73.
 36. Viaud S, Saccheri F, Mignot G, Yamazaki T, Daillère R, Hannani D, Enot DP, Pfirschke C, Engblom C, Pittet MJ, et al. The intestinal microbiota modulates the anticancer immune effects of cyclophosphamide. *Science.* 2013;342(6161):971–976. doi:10.1126/science.1240537.
 37. Dejea CM, Fathi P, Craig JM, Boleij A, Taddese R, Geis AL, Wu X, DeStefano Shields CE, Hechenbleikner EM, Huso DL, et al. Patients with familial adenomatous polyposis harbor colonic biofilms containing tumorigenic bacteria. *Science.* 2018;359(6375):592–597. doi:10.1126/science.aah3648.